S1. Crystal structural data of the DPPTO ligand

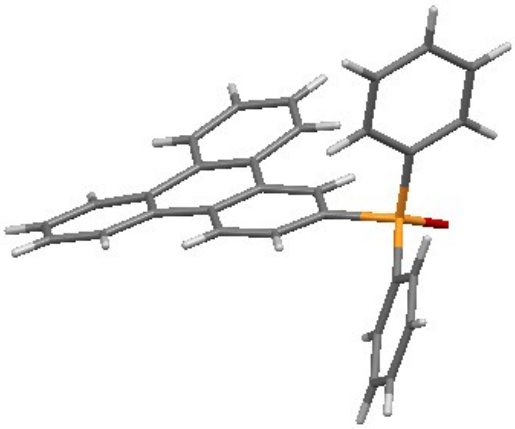

Figure S1 A crystal structure of the DPPTO ligand.

Table S1 Crystal data of DPPTO and $Eu(hfa)_3(DPPTO)_2$

	DPPTO	$Eu(hfa)_3(DPPTO)_2$
chemical formula	$C_{30}H_{21}OP$	$C_{75}H_{45}EuF_{18}O_8P_2$
formula weight	428.47	1630.02
crystal color, habit	colorless, platelet	colorless, needle
crystal system	monoclinic	monoclinic
space group	P 2_1/c	P 2_1/c
a / Å	15.1820(5)	13.1931(5)
b / Å	8.8000(3)	38.3635(14)
c / Å	16.1886(6)	13.7888(5)
α / deg	90.0000	90
β / deg	102.8661(13)	99.853(3)
γ / deg	90.0000	90
volume /Å	2108.52(13)	6876.0(4)
Z	4	4
density / g cm^{-3}	1.350	1.575
Temperature / °C	-150	20
μ (Mo Ka) / cm^{-1}	1.518	10.64
max 2θ / deg	54.9	28.93
Reflections	19514	64751
Independent refle	4807	15618
R	0.0370	0.0481
wR_2	0.1055	0.1217

S2. Photophysical properties of the DPPTO ligand

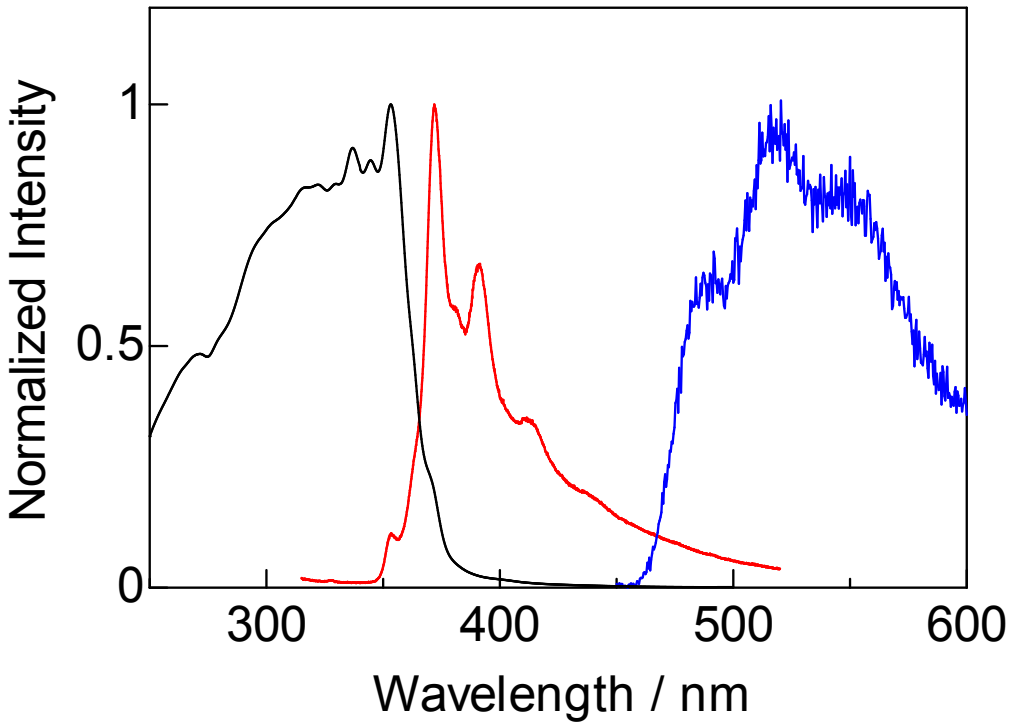

Figure S2. Electronic absorption (black line), fluorescence (red line, λ_{ex} = 350 nm), and phosphorescence (blue line, λ_{ex} = 350 nm, 90 K under vacuum) spectra of the DPPTO ligand in solid states.

S3. DFT calculation of the DPPTO ligand

TD-DFT calculations (B3LYP/6-31G(D)) were performed on the DPPTO ligand using the X-ray crystal structure. The calculated T_1 state mainly comprises five excited electronic configurations (HOMO-2→LUMO+2: 15 %, HOMO-1→LUMO: 29 %, HOMO-1→LUMO+1: 8 %, HOMO→LUMO: 9 %, HOMO→LUMO+1: 25 %). The electronic distribution of the related orbitals was almost localized on the triphenylene moiety (Figure S3).

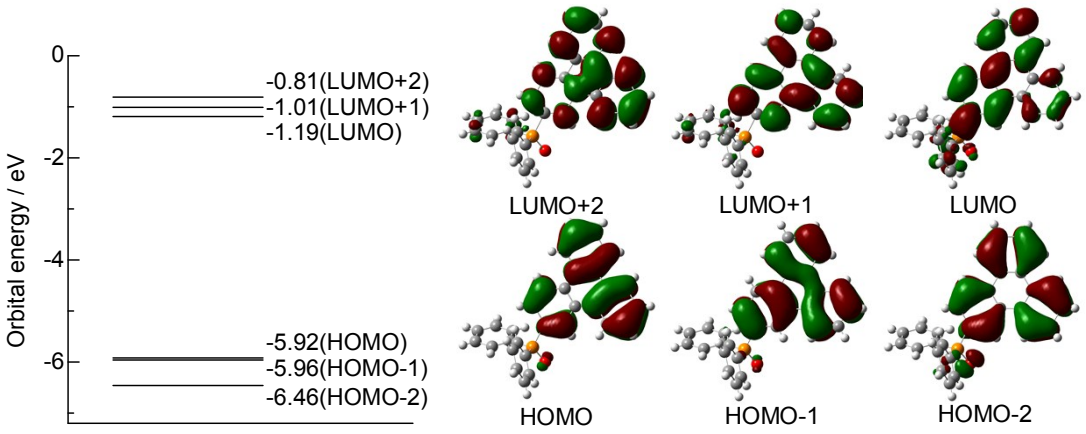

Figure S3. A molecular orbital energy diagram and molecular orbitals.

S4. Electronic absorption spectrum of the DPPTO ligand

The electronic absorption spectrum of the DPPTO ligand is shown in Figure S4. The peak wavelength (266 nm) of the DPPTO ligand is coincident with that of the $Eu(hfa)_3(DPPTO)_2$ (Figure S4). On the other hand, the absorption bandwidth becomes broad upon complexation, which might be caused by the ligand–ligand interaction in the $Eu(hfa)_3(DPPTO)_2$.

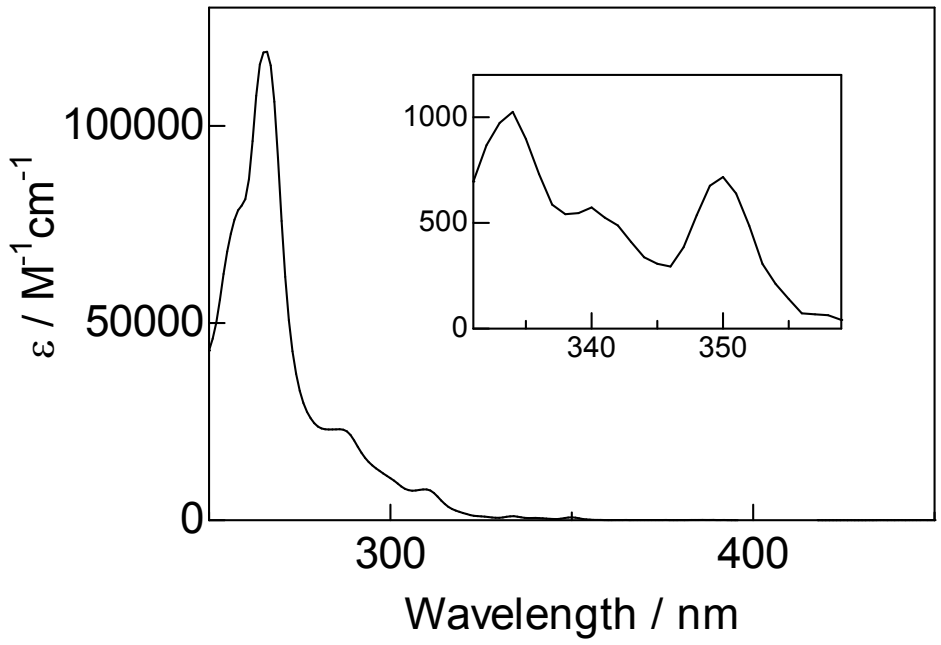

Figure S4. The electronic absorption spectrum of the DPPTO ligand in $CHCl_3$.

S5. Energy level diagram

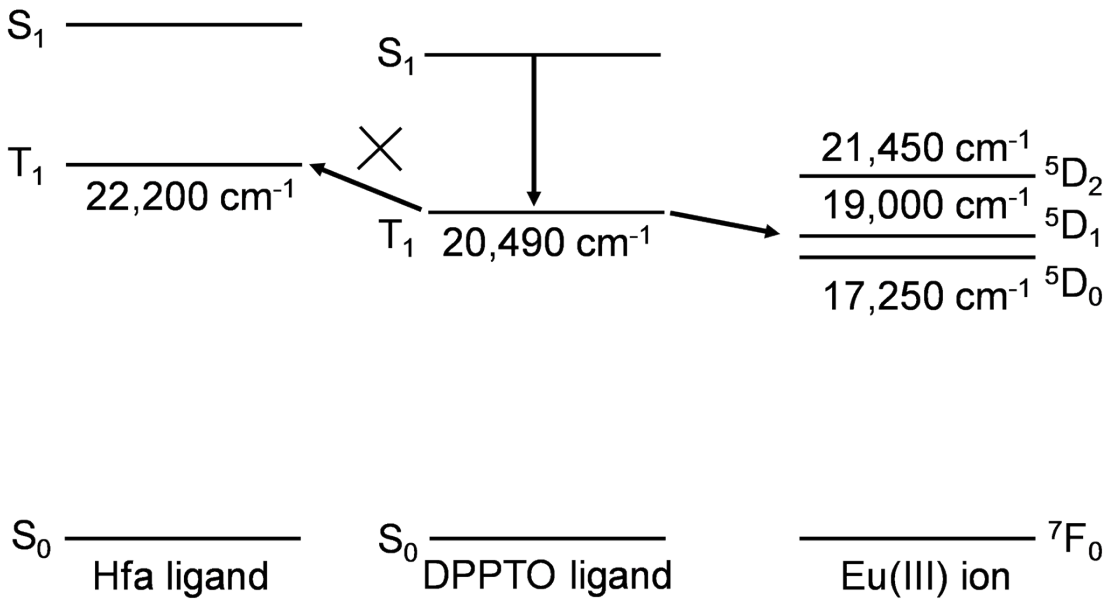

Figure S5. Energy level diagram of $Eu(hfa)_3(DPPTO)_2$ in solid state.

S6. Comparison of electronic absorption and excitation spectra of $Eu(hfa)_3(DPPTO)_2$

Figure S6 shows the electronic absorption spectrum of $Eu(hfa)_3(DPPTO)_2$ in a highly concentrated $CDCl_3$ solution (1×10^{-2} M) and the excitation spectrum of solid-state $Eu(hfa)_3(DPPTO)_2$. The spectra were normalized by the intensity maxima of the 4f–4f transition ($^7F_0 \rightarrow {}^5D_2$) band. The area ratios (A_{Ligand}/A_{Eu}) of the ligand and Eu(III) transition bands were calculated in which the numerator A_{Ligand} ranged from 400 to 460 nm and the denominator A_{Eu} ranged from 460 to 470 nm. The obtained A_{Ligand}/A_{Eu} ratio was only 11% lower in the absorption spectrum than in the excitation spectrum. The experimental results are consistent with the efficient energy migration (η_{sens} = 83%) from the ligands to Eu(III) ions in solid-state $Eu(hfa)_3(DPPTO)_2$.

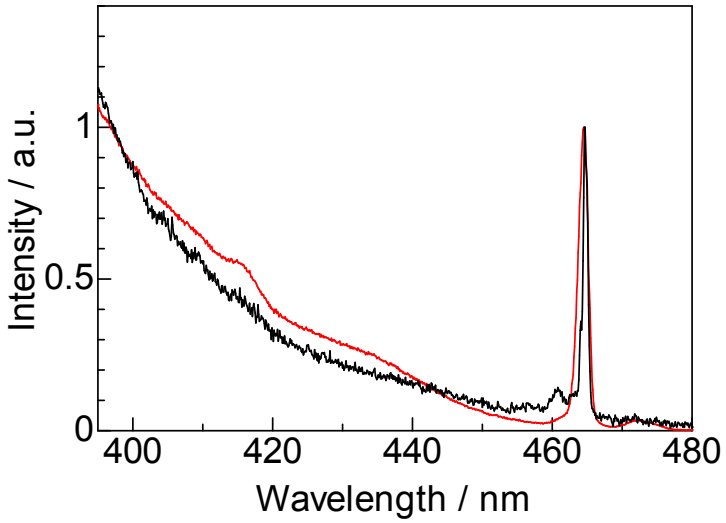

Figure S6. Electronic absorption spectrum (black line) of $Eu(hfa)_3(DPPTO)_2$ in $CDCl_3$ (1.0×10^{-2} M) and excitation spectrum (red line) of $Eu(hfa)_3(DPPTO)_2$ in the solid state.